

Accepted Manuscript

Upgrading coagulation with hollow-fibre nanofiltration for improved organic matter removal during surface water treatment

Stephan J. Köhler, Elin Lavonen, Alexander Keucken, Philippe Schmitt-Kopplin, Tom Spanjer, Kenneth Persson



PII: S0043-1354(15)30374-2

DOI: [10.1016/j.watres.2015.11.048](https://doi.org/10.1016/j.watres.2015.11.048)

Reference: WR 11675

To appear in: *Water Research*

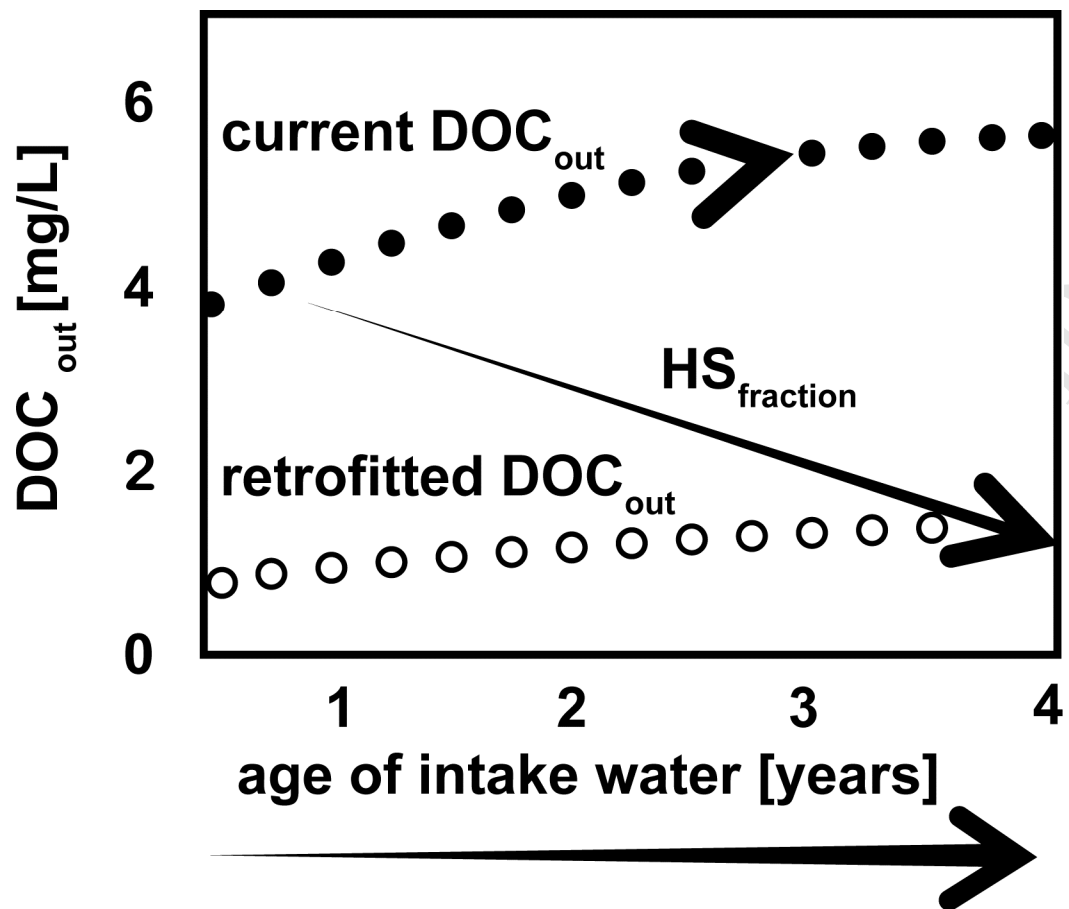
Received Date: 4 July 2015

Revised Date: 17 November 2015

Accepted Date: 20 November 2015

Please cite this article as: Köhler, S.J., Lavonen, E., Keucken, A., Schmitt-Kopplin, P., Spanjer, T., Persson, K., Upgrading coagulation with hollow-fibre nanofiltration for improved organic matter removal during surface water treatment, *Water Research* (2015), doi: 10.1016/j.watres.2015.11.048.

This is a PDF file of an unedited manuscript that has been accepted for publication. As a service to our customers we are providing this early version of the manuscript. The manuscript will undergo copyediting, typesetting, and review of the resulting proof before it is published in its final form. Please note that during the production process errors may be discovered which could affect the content, and all legal disclaimers that apply to the journal pertain.



1 **Upgrading coagulation with hollow-fibre nanofiltration for**
2 **improved organic matter removal during surface water**
3 **treatment**

4
5 Stephan J. Köhler^{1,*}, Elin Lavonen¹, Alexander Keucken^{2,3}, Philippe Schmitt-
6 Kopplin^{4,5}, Tom Spanjer⁶ and Kenneth Persson^{3,7}

7 ¹ Department of Aquatic Sciences and Assessment, Swedish University of Agricultural
8 Sciences, Box 7050, Uppsala, Sweden

9 ² Vatten & Miljö i Väst AB (VIVAB), Box 110, SE-311 22 Falkenberg, Sweden.

10 ³ Water Resources Engineering, Faculty of Engineering, Lund technical University, Box
11 118, SE-221 00 Lund, Sweden

12 ⁴ Analytical BioGeoChemistry, German Research Center for Environmental Health,
13 Helmholtz Zentrum München, 85764, Neuherberg, Germany

14 ⁵ Chair of Analytical Food Chemistry, Technische Universität München, 85354, Freising-
15 Weihenstephan, Germany

16 ⁶ Pentair X-Flow B.V., P.O. 739, 7500 AS Enschede, The Netherlands.

17 ⁷ Sydsvatten AB, Skeppsgatan 19, SE 211 19 Malmö, Sweden

18 *Corresponding author: stephan.kohler@slu.se

19 **Abstract**

20 Rising organic matter concentrations in surface waters in many Nordic countries require
21 current drinking water treatment processes to be adapted. Accordingly, the use of a novel
22 nanofiltration (NF) membrane was studied during a nine month period in pilot scale at a

23 large drinking water treatment plant in Stockholm, Sweden. A chemically resistant hollow-
24 fibre NF membrane was fed with full scale process water from a rapid sand filter after
25 aluminum sulphate coagulation. The combined coagulation and NF process removed more
26 than 90% of the incoming lake water dissolved organic carbon (DOC) (8.7 mg C L^{-1}), and
27 96% of the absorbance at 254 nm (A_{254}) (0.28 cm^{-1} incoming absorbance). Including
28 granulated active carbon (GAC) filter, the complete pilot plant treatment process we
29 observed decreases in DOC concentration (8.7 to 0.5 mg C L^{-1}), SUVA (3.1 to $1.7 \text{ mg}^{-1} \text{ L m}^{-1}$),
30 1), and the average nominal molecular mass (670 to 440 Da). Meanwhile, water hardness
31 was practically unaffected ($< 20\%$ reduction). Humic substances (HS) and biopolymers were
32 almost completely eliminated (6510 to 140 and 260 to $10 \text{ } \mu\text{g C L}^{-1}$ respectively) and low
33 molecular weight (LMW) neutrals decreased substantially (880 to $190 \text{ } \mu\text{g C L}^{-1}$).
34 Differential excitation emission matrices (EEMs), which illustrate the removal of
35 fluorescing organic matter (FDOM) over a range of excitation and emission wavelengths,
36 demonstrate that coagulation removed $35 \pm 2\%$ of protein-like material and $65 \pm 2\%$ of
37 longer emission wavelength, humic-like FDOM. The subsequent NF treatment was
38 somewhat less selective but still preferentially targeted humic-like FDOM ($83 \pm 1\%$) to a
39 larger extent than protein-like material ($66 \pm 3\%$). The high selectivity of organic matter
40 during coagulation compared to NF separation was confirmed from analyses with Fourier
41 transform ion cyclotron resonance mass spectrometry (FT-ICR-MS), and liquid
42 chromatography with organic carbon detection (LC-OCD), as coagulation exclusively
43 targeted oxidized organic matter components while NF removed both chemically reduced
44 and oxidized components. DOC removal and change in DOC character in the GAC filters
45 showed marked differences with slower saturation and more pronounced shifts in DOC
46 character using NF as pre-treatment. Fluorescence derived parameters showed a similar

47 decrease over time of GAC performance for the first 150 days but also indicated ongoing
48 change of DOM character in the post NF GAC filtrate over time even after LC-OCD
49 indicated steady state with respect to outgoing carbon. During our trial iron concentrations
50 were low (< 30 ppb) and thus A254 could be directly related to the concentration of HS ($R^2 =$
51 0.9). The fluorescence derived freshness index ($\beta:\alpha$) proved to be an excellent variable for
52 estimating the fraction of HS present in all samples. Given the recommended limit of 4 mg
53 L^{-1} for chemical oxygen demand (COD) for Swedish drinking water, coagulation will need
54 to be supplemented with one or more treatment steps irrespective whether climate change
55 will lead to drier or wetter conditions in order to maintain sufficient DOC removal with the
56 current increasing concentrations in raw waters.

57

58 **Keywords:** Nanofiltration (NF), Hollow fibre, Humic substances (HS), drinking
59 water, fluorescence EEM, GAC.

60 **1. Introduction**

61

62 Rising levels of dissolved organic matter (DOM) in boreal and north European surface
63 waters (Hongve *et al.* 2004,) pose a number of technical and chemical challenges for
64 drinking water production. Water treatment costs have increased and are expected to
65 continue to rise, especially when using coagulation techniques which require higher
66 chemical doses that results in more sludge (Eikebrokk *et al.* 2004). In addition, climate
67 change is expected to lead to larger fluctuations in dissolved organic carbon (DOC)
68 concentrations, commonly used as a proxy for DOM, and thus, further degradation of raw

69 water quality in the future (Delpla *et al.* 2009). Intensity, timing and duration of fluctuations
70 in DOC concentration and composition in surface waters are of vital economic interest for
71 drinking water producers but difficult to foresee. DOC removal through coagulation
72 treatment, which is the most commonly used method at Swedish water treatment plants
73 (WTPs), is affected by organic matter composition and the removal efficiency is commonly
74 reported to increase with the DOC-normalized absorbance at 254 nm (SUVA), an indicator
75 of aromatic carbon and a terrestrial origin (Matilainen *et al.* 2010, Weishaar *et al.* 2003).
76 The fraction of terrestrially derived DOC decrease with water turnover time in lakes
77 (Gondar *et al.* 2008, Tang *et al.* 2013, Köhler *et al.* 2013), leading to lowered removal
78 efficiency during the coagulation treatment. Lakes with varying turnover times are thus
79 more prone to temporal changes in DOC character. This is the case for Mälaren, the third
80 largest lake in Sweden, which is used as raw water source for three large WTPs supplying
81 the Swedish capital city Stockholm with drinking water. Raw water DOC concentration is
82 currently approximately 9 mg C L^{-1} , of which only roughly half can be removed through
83 coagulation treatment. Lake water retention time has been identified as a key driver of DOM
84 quality in this lake (Köhler *et al.* 2013, Lavonen *et al.* 2015). In Sweden, WTPs have to
85 comply with a recommended limit of around 4 mg C L^{-1} organic matter measured as
86 chemical oxygen demand (COD) for drinking water. In the case of Mälaren this is
87 equivalent to 5 mg C L^{-1} DOC. Future climate or land use driven changes in DOC
88 concentration and composition are thus large challenges for drinking water producers.
89 Lower outgoing DOC will lead to decreased unwanted consumption of disinfectant and,
90 reduced microbial regrowth potential in the distribution network. Improved DOC removal
91 prior to treatment with granular activated carbon (GAC) filters may furthermore decrease
92 fouling by irreversibly bound DOM components which diminish the ability of GAC filters

93 to remove micro-pollutants such as perfluorooctanesulfonic acid (PFOS), algal degradation
94 products or fuel residues, all which may occur in Mälaren.

95 High pressure (>10 bar), NF membranes with low molecular weight cut-off (< 300 Da) have
96 been used for a number years to remove organic matter for drinking water purposes (Meylan
97 *et al.* 2007). These tight membranes are efficient in removing DOC and hardness (e.g. Ca²⁺,
98 Mg²⁺, > 80% removal) as well as a number of organic micro-pollutants (Zhang *et al.* 2006).
99 Commercially available spiral wound NF membranes are designed for DOC removal at the
100 expense of undesirable retention of hardness for drinking water production from soft raw
101 waters. Furthermore, the spiral wound membranes are characterized by low chlorine
102 stability, limited disinfection and chemical cleaning possibilities, e.g. pH 3-8 for cellulose
103 acetate filters as compared to pH 2-12 for polysulfonate (Regula *et al.* 2014). Intensive pre-
104 treatment is necessary due to limited hydraulic cleaning options. Capillary, hollow fibre NF
105 membranes have been applied for direct filtration of highly colored surface water during the
106 last decade (Meylan *et al.* 2007). One of the latest concepts in NF for highly effective
107 removal of organic matter, the so called Color Removal Package, is based on capillary NF
108 membranes, combining the chemical resistance of hollow fibre membranes with the organic
109 carbon retention of spiral wound units (De Grooth 2015). These membranes are modified
110 for enhanced organic matter removal and limited retention of bivalent metal ions from the
111 feed water. As they are operated using outside in flow, they may be flushed inside out which
112 is ideal when retrofitting an existing treatment scheme. They do not require pretreatment
113 other than 300 micron safety screen and can directly be fed with raw surface water. In
114 summer 2013, a HFW 1000 membrane pilot plant was installed at Görväln WTP, situated in
115 Stockholm, Sweden, to evaluate the organic matter removal and performance of NF

116 filtration following conventional coagulation and rapid sand filtration. Organic matter
117 quality and quantity in all steps from raw to drinking water were evaluated with a large
118 range of analytical techniques. These included total and dissolved organic carbon (TOC,
119 DOC), online ultraviolet and visible (UV-VIS) absorbance (250-700nm), 3D fluorescence,
120 Fourier transform ion cyclotron resonance mass spectrometry (FT-ICR-MS) and liquid
121 chromatography with organic carbon detection (LC-OCD).

122 This study aims to a) evaluate the performance of a retrofitted new generation HFW 1000
123 nanofilter membrane, b) study the selective removal of DOM fractions in the combined
124 coagulation NF process and the currently used coagulation technique; c) identify DOM
125 characterization techniques that are informative for validating membrane and GAC
126 performance, and d) use the acquired data to estimate removal of DOC with varying
127 composition in the studied raw water as a function of lake water retention time.

128 **2. Material and methods**

129 **2.1 NF pilot plant**

130 The membrane material is composed of sulfonated polyether sulfone. The presence of
131 sulfonate groups on the benzene ring structure renders them hydrophilic and leads to a
132 negative zeta potential at pH above 5. The zeta potential further decrease to around -20 mV
133 with the raw water pH 7.5 used in our study and the membrane therefore effectively rejects
134 molecules with negatively charged functional groups such as DOC (De Grooth 2015). The
135 separating layer of the membrane is on the inside of the fibres, thus allowing operating
136 inside-out. The internal hydraulic diameter of the membrane fibers is 0.8 mm and the
137 molecular weight cut-off is approximately 1000 Da based on Dextran permeation.

138 The HFW 1000 NF membrane module is 0.20 m (8") in diameter and 1.54 m (60.5") long. It
139 contained 40 m² of membrane surface area with the 0.8 mm fibers. The test module was
140 equipped with surface flow collectors. The test facility (a QuickScan pilot plant, supplied by
141 Pentair X-Flow) had a capacity of 600 L h⁻¹ (permeate production). During the pilot trials
142 the test membrane was continuously operated at feed flow rate of 1.2 m³ h⁻¹ with a flux
143 range of around 15 L m⁻² h⁻¹, a cross-flow velocity of 0.5 m s⁻¹, an intermittent forward
144 flushing interval of every 60 minutes and a recovery rate of 50 %. We chose to protect the
145 membrane and operate at this low recovery even if higher recoveries of up to 80 were
146 successfully tested, With operating pressures around 4 bar and permeability rates of 10 L m⁻²
147 h⁻¹ bar⁻¹ the transmembrane pressure typically increased with 0.17 bar and the
148 permeability decreased with 1.0 L m⁻² h⁻¹ bar⁻¹ at low water temperatures of around 1-3 °C
149 during a filtration period of 42 days. The cleaning procedure is explained in detail in the
150 appendix.

151 **2.2 Mälaren as drinking water source**

152 Görvåln WTP is located in the eastern part, close to the outlet of Lake Mälaren, Sweden,
153 where water from a northern basin (16%) and the large western basin (84%) mix. Varying
154 water quality in the raw water intake is due to different processing of DOC within the lake
155 (Köhler *et al.* 2013). Mälaren raw water (2002-2013) has high pH (7.6-7.8), high alkalinity
156 (1.3 mM) and a DOC that varies between 6-12 mg L⁻¹. Raw water turbidity varies between 2
157 and 10 FNU depending on the raw water intake depth. A more detailed description of the
158 water quality and different water sources that contribute to the raw water at Görvåln WTP
159 can be found in Ericsson *et al.* 1984.

160 **2.3 Full scale drinking water plant**

161 The raw water (RAW) from Mälaren is taken in at two different intake depths (-4 and -22m)
162 depending on the water quality. After passing a micro sieve (200 μm nominal pore size) the
163 water is coagulated with $\text{Al}_2(\text{SO}_4)_3$ at doses varying from 40 to 70 mg L^{-1} . The coagulant
164 dose is controlled by measuring turbidity after the following rapid sand filtration (SF) (0.6
165 m h^{-1}), which is used to remove residual flocs. Downstream, the water is filtered through a
166 Norit 1240W GAC bed (CF), and disinfected with UV irradiation (25 mJ cm^{-2}) and
167 monochloramine (NH_2Cl ; 0.2-0.35 mg L^{-1}) to produce drinking water (DW) as shown on the
168 left side in Figure 1.

169 **2.4 Pilot scale drinking water treatment plant**

170 The feed water for the NF pilot plant water is recovered from the SF full-scale plant as
171 displayed in the right side of Figure 1. NF membrane module was followed by a pilot scale
172 GAC filter (CF2). A fraction of the rapid sand filtrate was filtered directly by another GAC
173 filter (CF4) so that the effect of NF on the activated carbon filter could be compared under
174 the same conditions regarding GAC age (Figure 1). Granulated activated carbon (GAC)
175 filter beads of approximately 2.5m height were filled with 1 m GAC (Norit 1240 W) and at
176 a hydraulic load of 10 m h^{-1} this resulted in an empty bed contact time of approximately 6
177 minutes at a flow rate of 1 L min^{-1} in accordance with the full scale plant conditions. This
178 setup was studied from August 2013 to May 2014.

179 **2.5 Online sensors**

180 The pilot plant was equipped with a number of sensors including an S:can absorbance probe
181 (spectro::lyser™; s::can Messtechnik GmbH), pH-meter, pressure transducers and a
182 conductivity probe. Absorbance spectra was acquired with the S:can sensor using a flow

183 through cell with 4cm path length in the wavelength range 230-750nm. Empirical
184 relationships from particle rich waters were used to calibrate the absorbance measurements
185 against both TOC and turbidity.

186 **2.6 Organic matter characterization**

187 Organic matter was characterized using a number of techniques. Regular and compulsory
188 samples monitoring the WTP performance ($n > 30$) between treatment steps were analyzed
189 for pH, alkalinity and UV absorbance at 254nm. S:can recorded absorbance spectra at the
190 raw water intake for the period July 2010 to June 2014 with one minute resolution.
191 Additionally, grab samples ($n = 20$) were analyzed for a number of DOC characteristics at
192 eight different sampling points throughout the drinking water train (Figure 1). Samples were
193 taken every month and at specific days prior to or after important adjustments in the setup,
194 such as change of active carbon in the filters or change of intake depth from level A to level
195 B (15.01.2013: 22 m \rightarrow 4m, 25.04.2013: 4m \rightarrow 22m, 04.02.2014: 22m \rightarrow 4m, and
196 25.02.2014: 4m \rightarrow 22m), shown as vertical lines in Figure A. 1. All samples were analyzed
197 for total and dissolved organic carbon (TOC and DOC) using a Shimadzu TOC-V_{CPH}. DOC
198 samples were filtered using pre-washed (MilliQ water, $< 18.2 \Omega \text{ cm}^{-1}$) cellulose acetate 0.45
199 μm filters (Minisart, Sartorius). Filter blanks were within 0.1 mg C L^{-1} of the DOC content
200 of MilliQ water. As TOC and DOC were always within the analytical precision of the
201 measurement (0.3 mg L^{-1}) we will only mention DOC in the subsequent text. Fluorescence
202 excitation emission matrices (EEMs) were collected using an Aqualog (Horiba Jobin Yvon)
203 spectrofluorometer (Lavonen *et al.* 2015). Previously established indices were calculated
204 from the corrected EEMs, namely HIX, fluorescence index (FI) and $\beta:\alpha$ according to Ohno
205 2002, Cory and McKnight 2005, and Parlanti *et al.* 2000. Changes in fluorescence spectra
206 over the whole measured range were assessed using differential EEMs (Lavonen *et al.*

207 2015) for the coagulation, NF and GAC treatments. To compare the removal of shorter
208 emission wavelength, protein-like autochthonous FDOM and longer emission wavelength,
209 terrestrially derived humic-like FDOM we looked at the % decrease in fluorescence signal
210 (differential EEM divided by measured EEM before a treatment process) at excitation = 276
211 nm, emission = 320 nm (protein-like) and excitation = 350 nm, emission = 550 nm (humic-
212 like). As the raw water was low in dissolved iron (< 30 ppb) and all treatment processes
213 studied here involved only small changes in pH ($6.6 < \text{pH} < 7.2$) we expect no significant
214 effect on the fluorescence spectra from the chemical conditions of the samples.

215 Approximately 1-20 L samples (depending on DOC concentration) were filtered through
216 pre-combusted (4 hours at 450 °C) GF/F filters (effective pore size of 0.7 μm) and acidified
217 to pH 2 using 37% HCl, p.a., before gravitationally loaded to solid phase extraction
218 cartridges (Agilent Bond Elut PPL). DOM was eluted with methanol according to Dittmar *et al.*
219 *al.* 2008. The methanol extracts were kept in a freezer until analyses were conducted.
220 Ultrahigh resolution MS analyses were performed at the Helmholtz Centre in Munich using
221 a 12 Tesla SOLARIX FT-ICR mass spectrometer (Bruker, Bremen, Germany) with an
222 Apollo II electrospray ionization source in negative ion mode. Chemical formulas were
223 assigned to the m/z peaks based on $^{12}\text{C}_{0-100}$, $^{16}\text{O}_{0-80}$, $^1\text{H}_{0-\infty}$, $^{14}\text{N}_{0-3}$, $^{32}\text{S}_{0-2}$. For further details
224 regarding FT-ICR-MS analyses, formula assignment and data processing, see Lavonen *et al.*
225 2015. Relative abundances of m/z peaks were calculated by dividing the signal intensities
226 by the intensity of the most abundant peak in each sample. Changes in relative abundance
227 during the different treatment processes are expressed in percentage points by subtracting
228 the relative abundance of an m/z peak in the sample after treatment from that in the sample
229 before treatment. Following Lavonen *et al.* 2015, where the same mass spectrometer was

230 used, we only considered changes in relative abundance by more than 2.5 percentage points
231 as significant, based on measurements of double samples where differences between signal
232 intensities were, on average, 0.9 ± 1.5 percentage points.

233 Liquid chromatograph organic carbon detection (LC-OCD) was used to analyze a large
234 number of samples ($n = 100$) from the pilot plant and the full scale process. LC-OCD
235 quantifies the elution as a function of size and column affinity of carbon and nitrogen from a
236 Sephadex column using a buffered ($\text{pH} = 6.85$ using a potassium-dihydrogenphosphate and
237 sodium-hydrogenphosphate buffer with an ionic strength of 2.5 mM) carrier solution (Huber
238 *et al.* 2011). This method has been calibrated using both standard IHSS and polystyrene
239 sulfonate standards and widely applied (Bagthoth *et al.* 2011). UV absorbance (254nm), C
240 and N are measured online, and allow quantifying the elution of DOC over time. The
241 acquired chromatogram is separated into different apparent size fractions using the
242 Chrom_CALC software (Huber *et al.* 2011) that divides DOC into the following apparent
243 size fractions as a function of elution time: Biopolymers, HS, building blocks, low
244 molecular weight neutrals and low molecular weight acids that are noted together as LMW.

245 **3. Results and discussion**

246 **3.1 Performance of the retrofitted NF pilot plant**

247 The pilot scale membrane plant produced treated water with constant water quality during
248 the whole 9 month experimental period, thus fulfilling one of the main objectives of the
249 study: stable removal of color and DOC over time. The stable DOC character is exemplified
250 by the data in Table 2 and 3 and Figure A.1 Both outgoing DOC concentration (0.6 ± 0.1 mg
251 C L^{-1}) and DOC character (i.e. $\beta:\alpha = 0.95 \pm 0.04$) of the NF permeate are very stable during
252 the whole study period. Raw water DOC concentration of around 8-11 mg C L^{-1} was

253 reduced to below 0.5 mg C L^{-1} after NF. Of this removal, the full scale coagulation
254 treatment accounted for approximately 50% while NF removed additionally 40% of the
255 DOC, only slightly lower than what can be achieved using conventional spiral wound
256 membranes (Meylan *et al.* 2007, Schafer *et al.* 2004, Metsamuuronen *et al.* 2014). In
257 contrast to the former membranes, the hollow fibre NF membranes used here succeeded to
258 retain less than 80% of incoming hardness (results not shown), as is desirable for soft raw
259 waters, thus avoiding a post-membrane alkalisation step. DOC concentration in the GAC
260 filter feed was significantly reduced (compare SF and NF-P in Table 2). Incoming DOC in
261 the water fed to the pilot plant GAC was eight times lower than that of the full scale GAC,
262 which was approximately 4 mg C L^{-1} . Across the whole pilot plant around 93% of incoming
263 HS, 86% of incoming DOC and 87% of A254 was removed.

264 **3.2 Selective removal of DOC across the whole and pilot plant treatment train**

265 **3.2.1 DOC concentration in the raw water**

266 Raw water DOC varied between 8.1 and 11.1 mg L^{-1} (10-90% quartiles respectively) during
267 our experiment period and was composed of approximately 70% HS (Table 2, Table A. 1
268 and Figure 2). The observed variation in DOC during the study period is thus very relevant
269 for dealing with the recently increasing raw water DOC (Figure A. 7) and for testing how
270 retrofitting a NF membrane may counteract this rise in DOC.

271 **3.2.2 Changes in DOC composition during coagulation**

272 DOC characterization using LC-OCD indicates that the coagulation treatment was, apart
273 from small quantities of large biopolymers, almost exclusively removing HS from the raw
274 water (Figure 2). A selective removal of UV-absorbing substances (Figure 2, SUVA in
275 Table 2) is in accordance with many previous studies (Baghoth *et al.* 2011, Shutova *et al.*

276 2014). Within the HS fraction, larger compounds were preferentially removed during the
277 coagulation step. Median nominal molecular weight for HS was 452 ± 30 Da after
278 coagulation, compared to 660 ± 70 Da in the incoming water (Table 2). Targeted removal of
279 larger components was also seen from the FT-ICR-MS data were the average nominal
280 molecular weight of CHO components that decreased significantly (were selectively
281 removed) was 440 Da (range from 302-578 Da) while the average mass for components that
282 increased significantly (were not/poorly removed) was 380 Da (range from 256-454 Da).
283 There was, furthermore, a clear shift in abundance from components with a positive average
284 carbon oxidation state to those with negative values (more reduced), in accordance with a
285 previous study of another WTP (Lovö) that also use eastern Mälaren as raw water source
286 and the same coagulation chemical as Görvåln WTP (Lavonen *et al.* 2015). Comparing the
287 components that decreased during coagulation at Görvåln and Lovö WTP formula by
288 formula showed that 82% (n=114) of those decreasing with >2.5 percentage points at
289 Görvåln also decreased significantly at Lovö despite being sampled different years and
290 seasons. This shows that coagulation is a rather stable process, repeatedly targeting similar
291 components. Differential EEMs indicate a strong preferential removal of terrestrial FDOM
292 with emission at long wavelengths (Figure 3 and Figure A. 4), as demonstrated by low $\beta:\alpha$
293 (0.48 ± 0.01) and FI 1.37 ± 0.02 , and HIX close to 1 (0.94 ± 0.01) for the calculated
294 removed fraction (Table 3), in line with Lavonen *et al.* 2015. Removal ranged from $35 \pm 2\%$
295 for protein-like material to $65 \pm 2\%$ of longer emission wavelength, terrestrially derived
296 FDOM (Figure 3, left).

297 **3.2.3 GAC in full and pilot scale**

298 Detailed analysis of full scale or pilot scale long term experiments involving GAC filters are
299 rare (Gibert *et al.* 2013). In the full scale treatment Görvåln WTP aims to use their GAC

300 filter as a chemical barrier. However, due to the relatively high DOC concentration in the
301 GAC feed ($4.8 \pm 0.3 \text{ mg C L}^{-1}$), the filters commonly become saturated with irreversibly
302 bound DOM compounds within 1 month after regeneration (Matilainen *et al.* 2006) and do
303 not remove any DOC (Table A. 1). The current GAC thus functions as a biofilter, where
304 microbes adsorbed to the GAC surface remove e.g. compounds causing taste and odor, and
305 in some case smaller amounts of DOC e.g. (Camper 2004, Matilainen *et al.* 2006, Gibert *et*
306 *al.* 2013). The pilot reference GAC filter (CF4) reduced 75% of the incoming DOC when
307 the activated carbon was new, but after being used for just 1 month the removal had been
308 lowered to 11% (0.5 mg C L^{-1}). After one additional month until the end of the experiment
309 period hardly any ($0.1 \pm 0.8 \text{ mg C L}^{-1}$) was removed (Figure A. 6). The pilot GAC filter that
310 was fed with NF permeate (CF2) showed a similar reduction in DOC removing capacity
311 over time with the largest removal when the activated carbon was new ($72\% = 1.4 \text{ mg C L}^{-1}$
312 $^{-1}$), which decreased to 0.5 mg C L^{-1} removal the next coming two months and thereafter the
313 reduction in DOC was only 0.1 mg C L^{-1} until the end of the trial period, similar to CF4.
314 Both GAC filters in the pilot plant initially removed large amount of both humic-like (77
315 and 96% for CF4 and CF2 respectively) and protein-like FDOM (70 and 61% respectively)
316 (Figure 4, left panel). Our LC-OCD analysis confirmed the results from Gibert *et al.* 2013
317 who also observed preferential removal of HS during the early phase (Figure 4, right panel).
318 The Norit 1240 W seems to have a higher affinity for HS than Norit Row 0.8 supra used in
319 (Gibert *et al.* 2013 under the given conditions. This was not studied further but could be due
320 to differences in water quality such as pH, presence of cations that change the conformation
321 of HS in solution (Schafer, 2004) and differences in the GAC pore size distribution.
322 According to Camper 2004, HS may support the same amount of microbial growth in a
323 biofilm as readily available smaller LMW substances. Even if no change in DOC could be

324 quantified across the full scale GAC filter, there was still a clear pattern in FDOM removal
325 demonstrated by a decrease in $15 \pm 11\%$ for protein-like material and $3 \pm 1\%$ for humic-like
326 material, indicating that the GAC mainly had acted as a biofilter as humic material primarily
327 is removed through adsorption (Velten *et al.* 2011, Matilainen *et al.* 2006): Both
328 fluorescence and LC-OCD data are thus valuable for indicating changes in GAC saturation
329 and functioning.

330 **3.2.4 Changes in DOC concentration and composition across the NF membrane**

331 In the pilot plant 40% of the incoming DOC was removed with the NF membrane. The two
332 main fractions that were retained (>90%) were biopolymers and HS (Figure 2). Similar or
333 higher removals are observed in tighter spiral wound membranes (Schafer *et al.* 2004) and
334 (Meylan *et al.* 2007). Up to 80% of the smaller constituents - building blocks and low
335 molecular weight compounds were removed (Table 2, Table A. 1). UV absorbing
336 compounds were removed slightly more than bulk DOC with SUVA decreasing from 2.1 to
337 1.7 (Table 2). This and the significant increase in FI and $\beta:\alpha$ during membrane treatment
338 demonstrates selective removal of terrestrial DOM (Table 3). FI in the treated water was
339 1.84 ± 0.03 which indicates that so much terrestrial DOM was removed in the combined
340 coagulation NF treatment that the permeate (Table 3) resembled organic compounds from
341 extracellular release and leachate from algae and bacteria defined as a microbial endmember
342 (McKnight *et al.* 2001). Even if NF was selectively removing terrestrial DOM, indices
343 calculated from differential EEMs show that the removed DOC still had a rather microbial
344 fingerprint (high FI (1.64 ± 0.02) and $\beta:\alpha$ (0.71 ± 0.02)). This demonstrates that NF can
345 remove a wide range of DOM components, reflected in $83 \pm 1\%$ removal of humic-like
346 FDOM and $66 \pm 3\%$ reduction in protein-like material (Figure 3). This is supported by FT-
347 ICR-MS results, showing that more than 90% of the components that decreased

348 significantly in relative abundance during coagulation ($n = 139$) further decreased with NF.
349 Also, 93 components that were not targeted during coagulation decreased significantly
350 during NF. The coagulation treatment was highly selective towards oxidized components
351 with a weighted (against the relative abundance) mean average carbon oxidation state (
352 **Error!**) of 0.35 for decreasing components (maximum 0.78 and minimum -0.10 for
353 components that decreased significantly). Meanwhile, NF removed a wider range of both
354 reduced and oxidized components (weighted mean **Error!** = -0.05, maximum 0.63 and
355 minimum -0.61 for components decreasing significantly). Hence, we can show that NF with
356 the employed membrane is more efficient than coagulation, both continuing to remove
357 material reactive during coagulation, as well as additional components. All components that
358 increased in relative abundance during NF treatment had $m/z < 400$ Da (Figure 5). This
359 indicates that these components do not aggregate significantly and have therefore not been
360 removed through size exclusion. There were also components that had $m/z < 400$ Da that
361 decreased in abundance, however, these had significantly higher O/C (> 0.50) (right panel in
362 Figure 5). A higher removal of smaller but highly charged molecules is in line with
363 expected repulsion on negatively charged membranes (Schafer *et al.* 2004).

364 **3.3 Identifying useful spectroscopic information for DOC character**

365 From August 2012 the S:can was used to control the $\text{Al}_2(\text{SO}_4)_3$ dosing for improved DOC
366 removal in the full scale WTP. From then on dosing efforts were increased and controlled
367 by the online UV signal. Two thirds of HS were removed using a coagulant dose of around
368 50 mg/l $\text{Al}_2(\text{SO}_4)_3$. The removed DOC was almost entirely composed of HS (96%) (Figure
369 2). This explains why the relative removal of DOC is well correlated to both %HS, Al_{DOS}
370 and to A254 (Table 1). On average, the online sensor controlled dosing was higher than the
371 turbidity controlled dosing (75 versus 50 mg L⁻¹ $\text{Al}_2(\text{SO}_4)_3$ and led to a 12% higher DOC

372 removal (around 1 mg L^{-1} on average). Controlling the coagulant dose with absorbance
373 measured online will allow the WTP to remove more DOC under periods with high A254
374 when DOC is easy to coagulate as shown below.

375 Due to the importance of HS for DOC removal during coagulation we analyzed whether any
376 of the optical parameters could be coupled to the LC-OCD data. When comparing the
377 average $\beta:\alpha$ with average fraction of HS of total DOC in the raw water, rapid sand filtrate
378 and NF permeate and concentrate as well as the drinking water we obtained a linear
379 relationship (Figure 6). Using average data (Table 3) from delta EEMs from raw water to
380 coagulation (RAW/SF) and from coagulation to NF (SF/NF-P) we may produce two
381 additional data points using mass balance calculations of changes in HS (Figure 6). There
382 were a number of other interesting relationships (e.g. prediction of molecular weight of HS
383 as a function of increasing HIX, HS as a function of A254 (Table 1) in line with the results
384 of (Baghoth *et al.* 2011). We focused on another important aspect for finished drinking
385 water, notably the presence of low molecular weight compounds (LMW) in the permeate. In
386 our study we found that LMW determined by LC-OCD in the permeate may be estimated
387 from HIX and $\beta:\alpha$ (Figure A. 6). In line with Baghoth *et al.* 2011 and Baker *et al.* 2008 our
388 results confirm that fluorescence signals may be coupled to NOM properties.

389 Both GAC and membrane performance may thus be followed using fluorescence as a faster
390 and cheaper indicator of DOC quality on site. While these relationships (e.g. UV versus
391 DOC (Figure A. 2), DOC versus building blocks etc.) are useful for individual WTPs, we
392 agree with Shutova *et al.* 2014 that further work is needed to exclude that they are only site
393 specific. Complicating factors in such an analysis would be the presence of dissolved iron
394 (Weishaar *et al.* 2003), pH (Pace *et al.* 2012) and presence of cations (Schafer *et al.* 2004)

395 that all may influence absorbance and fluorescence due to either changes in organic matter
396 conformation or metal binding.

397 **3.4 Effect of lake water retention time on coagulation efficiency as one aspect of** 398 **climate adaptation**

399 Both Gondar *et al.* 2008 and Köhler *et al.* 2013 have noted that lake water NOM may be
400 described as two endmembers that are mainly controlled by lake turnover and flow. Dry
401 spells may have a significant effect of lake water quality as lake water NOM during those
402 periods usually contain more hydrophilic NOM (Tang *et al.* 2013, Ritson *et al.* 2014) and
403 less of hydrophobic HS. Removal of incoming DOC during coagulation treatment is
404 controlled by the fraction of HS present in the raw water. The abundance of HS can be
405 estimated from A254 (Figure A. 3). A254 is, however, affected by the presence of iron
406 (Weishaar *et al.* 2003) and during periods of high iron concentrations (> 300ppb) as was
407 observed in the year 2000 (personal communication Görvåln WTP) this relationship will
408 fail. Both $\beta:\alpha$ and DOC concentration, however, have previously been shown (Figure 6) to
409 be controlled by lake water retention time (Köhler *et al.* 2013) This information could be
410 combined to estimate how shorter or longer lake water retention times may control raw
411 water DOC concentrations and $\text{Al}_2(\text{SO}_4)_3$ doses. Using a series of linear regression that
412 relate age with DOC and $\beta:\alpha$ (Figure 7), $\beta:\alpha$ with HS (Figure 6) and HS with dosing and
413 DOC removal (Table 1) we may estimate outgoing DOC from raw water DOC and $\beta:\alpha$ that
414 both change with the age of incoming raw water. As $\beta:\alpha$ proved to be an excellent indicator
415 of the percentage of HS present, we selected this optical variable to further evaluate its
416 usefulness to assess coagulation treatability of DOM. Two different scenarios with varying
417 water age as surrogates for high respective low flow conditions and varying DOC
418 concentration and their respective $\beta:\alpha$ and %HS are displayed in Figure 7. Despite varying

419 incoming DOC in our scenario (7-14 mg C L⁻¹), drinking water DOC is expected to vary
420 between 3.3 and 4.7 requiring Al₂(SO₄)₃ doses between below 10 to almost 100 mg L⁻¹,
421 twice the average dose used today. Wet years with short lake WRT (< 1 year) will lead to
422 exceptionally high Al₂(SO₄)₃ dosing due to the increased presence of HS while dry years
423 with long WRT (> 3 years) will lead to low Al₂(SO₄)₃ dosing but almost similar outgoing
424 DOC. Should the current observed trend of increasing DOC that has been recorded at the
425 outlet of Mälaren (Figure A. 7), and large areas of Sweden and Norway continue for several
426 years, outgoing DOC will be above 5 mg L⁻¹ irrespective of the chosen scenario.

427 Another important question of interest is how the fraction of hydrophilic and neutral
428 DOC giving rise to biologically degradable organic carbon will vary in the future. The most
429 relevant fraction is probably that determined as LMW through LC-OCD. Applying the
430 regression in Figure A. 6 and using lake water HIX and β/α LMW decreases from 0.8 to 0.6
431 mg L⁻¹ across the lake. Lake water retention time thus only has a minor effect on LMW.
432 Future studies will need to address that question in more detail.

433 **3.5 Remaining questions and challenges with hollow fibre membrane filtration**

434 Fluorescence EEMs and LC-OCD analyses indicate that the NF permeate consists of
435 microbial derived low molecular weight components, rich in organic nitrogen that might
436 affect the biological activity (regrowth potential) and chemical reactivity (disinfectant
437 stability, corrosion of pipes) in the distribution network. There are recurrent algal blooms in
438 Mälaren and the lake also receives waste water from a number of smaller cities and one
439 large hospital within the catchment. The NF membrane used in this study would allow
440 removing at least some of the larger hydrophilic micropollutants such as microcystines and
441 large PFCAs (Perfluorodecanoate 513 Da) and PFOS (Perfluorooctane sulfonic acid 500

442 Da). Other typically occurring, smaller compounds such as ketoprofene ($pK_a = 4.5$, 250 Da),
443 or danofloxazine ($pK_a = 6.0$, 360 Da) might permeate. In the future we will analyze the fate
444 of a number of micro pollutants through today's and the new proposed water treatment train
445 to test the ability of NF to either retain or improve the removal efficiency of GAC filters.

446 **4. Conclusions**

447 Improved removal of organic matter from surface water is important for surface waters in
448 Nordic countries that currently undergo show increasing trends of organic carbon.
449 Stockholm produces its drinking water from raw water ($DOC = 9 \text{ mg L}^{-1}$) taken in Mälaren,
450 Sweden's third largest lake. DOC has increased over the last 19 years from 6 to 10 mg L^{-1}
451 and we expect larger temperature and flow driven variations in DOC concentration and
452 character over time in the future. At current full scale operation using aluminum coagulation
453 indicate removal of larger ($> 500 \text{ Da}$ and HS only) terrestrial ($FI = 1.4$, $\beta:\alpha = 0.5$) and with a
454 higher mean average carbon oxidation state (**Error!** = 0.5) carbon. Using $\beta:\alpha$ that relates to
455 the presence of HS in the studied water we may estimate the outgoing DOC concentration as
456 a function of incoming DOC character in the incoming water based on established
457 coagulation dose DOC and colour relationships. The existing aluminum coagulation
458 (outgoing $DOC = 4.5 \text{ mg C L}^{-1}$) and granular active carbon (outgoing $DOC = 4.0 \text{ mg C L}^{-1}$)
459 process alone might not be able to handle these future changes. Longer water retention times
460 during dry spells will decrease the fraction of hydrophobic DOC that is easy to flocculate.
461 We chose to use a novel and more resistant hollow-fibre polysulfone nanofilter (HFW 1000)
462 instead of spiral wound membranes as they would affect hardness too much in the studied
463 soft waters. The coupled coagulation-NF pilot plant produced stable outgoing water quality
464 (0.5 mg L^{-1}) during the nine month test trial. The removal of carbon with a much larger

465 range of size (350-500 Da) and properties (**Error!**= -0.07, FI = 1.65, $\beta:\alpha = 0.5$) during NF as
466 compared to coagulation was confirmed using a large array of methods including LC-OCD,
467 FT-ICR-MS and fluorescence. Even if the fluorescence derived parameters and correlations
468 probably are site specific they are reliable, fast to determine and comparably cheap
469 complement to the more advanced techniques used here (FT-ICR-MS and LC-OCD). DOC
470 removal and change of DOC character in the GAC filters in full scale, the current
471 coagulation scheme and pilot plant setup showed marked differences with slower saturation
472 and larger changes in DOC character using fresh GAC. The removal of potentially elevated
473 concentrations of organic contaminants such as diesel, microcystines or persistent organic
474 micropollutants in Mälaren may thus improve using the proposed new scheme.

475 **5. Acknowledgements**

476

477 Chemical analysis and the working time of S.J, Köhler was financed by two research grants, grant
478 number 11-112 Genomembran and through the research network DRICKS that are financed by the
479 Swedish Water and waste water association. Elin Lavonen was financed through the FORMAS grant
480 Color of water.

481 **6. References**

482

483 Baghoth, S.A., Sharma, S.K. and Amy, G.L. (2011) Tracking natural organic matter (NOM)
484 in a drinking water treatment plant using fluorescence excitation-emission matrices and
485 PARAFAC. *Water Research* 45(2), 797-809.

- 486 Baker, A., Tipping, E., Thacker, S.A. and Gondar, D. (2008) Relating dissolved organic
487 matter fluorescence and functional properties. *Chemosphere* 73(11), 1765-1772.
- 488 Camper, A.K. (2004) Involvement of humic substances in regrowth. *Int J Food Microbiol*
489 1(92(3)), 355-364.
- 490 Cory, R.M. and McKnight, D.M. (2005) Fluorescence spectroscopy reveals ubiquitous
491 presence of oxidized and reduced quinones in dissolved organic matter. *Environ. Sci.*
492 *Technol.* 39(21), 8142-8149.
- 493 De Grooth, J. (2015) A Tale Of Two Charges: Zwitterionic Polyelectrolyte Multilayer
494 Membranes. Ph.D., Twente University, Twente.
- 495 Dittmar, T., Koch, B., Hertkorn, N. and Kattner, G. (2008) A simple and efficient method
496 for the solid-phase extraction of dissolved organic matter (SPE-DOM) from seawater.
497 *Limnology and Oceanography: Methods* 6, 230-235.
- 498 Eikebrokk, B., Vogt, R.D. and Liltved, H. (2004) NOM increase in Northern European
499 source waters: discussion of possible causes and impacts on coagulation/contact filtration
500 processes. *Water Science and Technology* 4(4), 47-54.
- 501 Ericsson, P., Hajdu, S. and Willén, E. (1984) Vattenkvaliteten i Görvälän. En dynamisk
502 Mälarfjärd. Vattenkemi och växtplankton i ett fyrtioårigt perspektiv (in Swedish). *Vatten*
503 40, 193-211.
- 504 Gibert, O., Lefevre, B., Fernandez, M., Bernat, X., Paraira, M. and Pons, M. (2013)
505 Fractionation and removal of dissolved organic carbon in a full-scale granular activated
506 carbon filter used for drinking water production. *Water Research* 47(8), 2821-2829.

- 507 Gondar, D., Thacker, S., Tipping, E. and Baker, A. (2008) Functional variability of
508 dissolved organic matter from the surface water of a productive lake. *Wat. Res.* 42(1-2), 81-
509 90.
- 510 Hongve, D., Riise, G. and Kristiansen, J.F. (2004) Increased colour and organic acid
511 concentrations in Norwegian forest lakes and drinking water – a result of increased
512 precipitation? *Aquatic Sciences* 66, 231-238.
- 513 Huber, S.A., Balz, A., Abert, M. and Pronk, W. (2011) Characterisation of aquatic humic
514 and non-humic matter with size-exclusion chromatography - organic carbon detection -
515 organic nitrogen detection (LC-OCD-OND). *Water Research* 45(2), 879-885.
- 516 Köhler, S.J., Kothawala, D., Futter, M.N., Liungman, O. and Tranvik, L. (2013) In-Lake
517 Processes Offset Increased Terrestrial Inputs of Dissolved Organic Carbon and Color to
518 Lakes. *Plos One* 8(8).
- 519 Lavonen, E.E., Kothawala, D.N., Tranvik, L.J., Gonsior, M., Schmitt-Kopplin, P. and
520 Köhler, S.J. (2015) Ultra-high resolution mass spectrometry explains changes in the optical
521 properties of dissolved organic matter during drinking water production (in review for
522 *Water Research*)
- 523 Matilainen, A., Vepsäläinen, M. and Sillanpää, M. (2010) Natural organic matter removal
524 by coagulation during drinking water treatment: A review. *Advances in Colloid and*
525 *Interface Science* 159(2), 189-197.
- 526 Matilainen, A., Vieno, N. and Tuhkanen, T. (2006) Efficiency of the activated carbon
527 filtration in the natural organic matter removal. *Environment international* 32(3), 324-331.

- 528 McKnight, D.M., Boyer, E.W., Westerhoff, P.K., Doran, P.T., Kulbe, T. and Andersen, D.T.
529 (2001) Spectrofluorometric characterization of dissolved organic matter for indication of
530 precursor organic material and aromaticity. *Limnology and Oceanography* 46(1), 38-48.
- 531 Metsamuuronen, S., Sillanpaa, M., Bhatnagar, A. and Manttari, M. (2014) Natural Organic
532 Matter Removal from Drinking Water by Membrane Technology. *Separation and*
533 *Purification Reviews* 43(1), 1-61.
- 534 Meylan, S., Hammes, F., Traber, J., Salhi, E., von Gunten, U. and Pronk, W. (2007)
535 Permeability of low molecular weight organics through nanofiltration membranes. *Water*
536 *Research* 41(17), 3968-3976.
- 537 Ohno, T. (2002) Fluorescence inner-filtering correction for determining the humification
538 index of dissolved organic matter. *Environmental Science & Technology* 36(4), 742-746.
- 539 Pace, M., Reche, I., Cole, J., Fernández-Barbero, A., Mazuecos, I. and Prairie, Y. (2012) pH
540 change induces shifts in the size and light absorption of dissolved organic matter.
541 *Biogeochemistry* 108(1-3), 109-118.
- 542 Parlanti, E., Worz, K., Geoffroy, L. and Lamotte, M. (2000) Dissolved organic matter
543 fluorescence spectroscopy as a tool to estimate biological activity in a coastal zone
544 submitted to anthropogenic inputs. *Organic Geochemistry* 31(12), 1765-1781.
- 545 Regula, C., Carretier, E., Wyart, Y., Gesan-Guiziou, G., Vincent, A., Boudot, D. and
546 Moulin, P. (2014) Chemical cleaning/disinfection and ageing of organic UF membranes: a
547 review. *Water Res* 56, 325-365.

- 548 Ritson, J.P., Graham, N.J.D., Templeton, M.R., Clark, J.M., Gough, R. and Freeman, C.
549 (2014) The impact of climate change on the treatability of dissolved organic matter (DOM)
550 in upland water supplies: A UK perspective. *Science of the Total Environment* 473, 714-
551 730.
- 552 Schafer, A.I., Pihlajamaki, A., Fane, A.G., Waite, T.D. and Nystrom, M. (2004) Natural
553 organic matter removal by nanofiltration: effects of solution chemistry on retention of low
554 molar mass acids versus bulk organic matter. *Journal of Membrane Science* 242(1-2), 73-
555 85.
- 556 Shutova, Y., Baker, A., Bridgeman, J. and Henderson, R.K. (2014) Spectroscopic
557 characterisation of dissolved organic matter changes in drinking water treatment: From
558 PARAFAC analysis to online monitoring wavelengths. *Water Research* 54, 159-169.
- 559 Tang, R., Clark, J.M., Bond, T., Graham, N., Hughes, D. and Freeman, C. (2013)
560 Assessment of potential climate change impacts on peatland dissolved organic carbon
561 release and drinking water treatment from laboratory experiments. *Environmental Pollution*
562 173, 270-277.
- 563 Velten, S., Knappe, D.R.U., Traber, J., Kaiser, H.-P., von Gunten, U., Boller, M. and
564 Meylan, S. (2011) Characterization of natural organic matter adsorption in granular
565 activated carbon adsorbers. *Water Research* 45(13), 3951-3959.
- 566 Weishaar, J.L., Aiken, G.R., Bergamaschi, B.A., Fram, M.S., Fujii, R. and Mopper, K.
567 (2003) Evaluation of specific ultraviolet absorbance as an indicator of the chemical
568 composition and reactivity of dissolved organic carbon. *Environmental Science &*
569 *Technology* 37(20), 4702-4708.

570 Zhang, Y., Causserand, C., Aimar, P. and Cravedi, J.P. (2006) Removal of bisphenol A by a
571 nanofiltration membrane in view of drinking water production. *Water Research* 40(20),
572 3793-3799.

573

ACCEPTED MANUSCRIPT

574 **Dummy Figures and tables:**

575 Figure 1. Water treatment train for the full scale drinking water plant and the pilot scale
576 drinking water plant at Görvåln waterworks. The codes for raw water (RAW), sand filter
577 (SF), full scale active carbon filter (CF), nanofilter concentrate (NF-C), nanofilter permeate
578 (NF-P), the other two carbon filters (CF2 and CF4) and drinking water (DW) are used
579 throughout the paper

580 Figure 2. Selected results of median values for changes in DOC [ppb] quantity and quality
581 across the WTP and pilot plant from the raw water (RAW) through the sand filter (SF), the
582 nanofilter (NF-P) and through the full scale activated carbon (SF-CF4) to the final drinking
583 water (DW) and after the activated carbon filter of the pilot plant (NF-CF2) for all samples
584 in the period August 2013 to June 2014. DOC quality parameters in order of decreasing
585 molecular size are codes as biopoly = Biopolymers, HS = Humic substances; LMW = low
586 molecular weight neutrals; build = building blocks.

587 Figure 3 Fraction of removed fluorescent dissolved organic matter for coagulation (left) and
588 NF (right) treatments. Dark red colors indicate strong removal ($> 75\%$) while blue-purple
589 colors indicate less removal ($< 40\%$). The excitation/emission wavelength pairs chosen to
590 represent humic-like ($E_x = 350$ nm, $E_m = 550$ nm, marked "H" in the EEMs) and protein-
591 like ($E_x = 276$ nm, $E_m = 320$ nm, marked "P" in the EEMs).

592 Figure 4 Removal (left panel) of protein-like (triangles) and humic-like (circles) fluorescent
593 dissolved organic matter and (right panel) removal of low molecular neutrals (triangles),
594 humic substances (circles), building blocks (diamonds) and biopolymers (squares) across
595 granulated activated carbon (CF) filters in the full scale treatment (black symbols), as well

596 as the pilot plant reference (CF4, white symbols), and downstream from the NF membrane
597 (CF2, grey symbols).

598 Figure 5 CHO components that increased (left) and decreased (right) during the pilot scale
599 nanofiltration of, with chemical coagulation, treated water. White and black bubbles
600 demonstrate significant changes in relative abundance while gray bubbles show non
601 significant changes. Bubble size represent the magnitude of the change in relative
602 abundance (maximum 52 percentage points decrease and 24 percentage points increase).

603 Figure 6 Left: Measured fraction of humic substances (HS_{frac}) for Raw, SF, DW and NF-P
604 as a function of $\beta:\alpha$ (black diamonds) and mass balance derived HS_{frac} for the material that
605 was removed during coagulation and NF treatments versus $\beta:\alpha$ calculated from differential
606 EEM (white diamonds). The regression line is very close to that estimated from all
607 individual data shown to the right. HS_{frac} (predicted) was estimated using $\beta:\alpha$ ($HS_{frac} = 1.52$
608 $- 1.33 * \beta:\alpha$) for all samples except CF2 where DOC concentrations were low.

609 Figure 7 Measured and fitted DOC and $\beta:\alpha$ across Mälaren as a function of water age to the
610 left (Data from Köhler et al 2013). Black circles and black stars display measured DOC and
611 measured $\beta:\alpha$ respectively (left panel). Both DOC and $\beta:\alpha$ are read out as a function of water
612 age (x-axis in left panel) using the horizontally pointing arrows in the left panel. On the
613 right: predicted fraction of DOC composed of HS (HS_{frac}) (x-axis) estimated from as a
614 function of incoming $\beta:\alpha$ (left y-axis) (black stars) and DOC (right y-axis) (black circles)
615 using eqs. 2,3, and 8 in Table A. 1 that relate $\beta:\alpha$, HS, DOC and aluminum dose. Vertically
616 downwards pointing arrows indicate the amount of DOC (difference between black and
617 white circles) that can be removed through coagulation treatment for two different situations
618 (A and B); The predicted outgoing DOC (white circles in the right panel) is illustrated for A

619 (a “young” water 0.7 months of age with high DOC and high $HS_{\text{frac}} = 0.8$, requiring around
620 $90 \text{ mg L}^{-1} \text{ Al}_2(\text{SO}_4)_3$ and outgoing DOC of around 3.3 mg L^{-1}) and B (an “old water” with
621 lower DOC, lower $HS_{\text{frac}} = 0.65$ leading to a low dose of $40 \text{ mg L}^{-1} \text{ Al}_2(\text{SO}_4)_3$ and outgoing
622 DOC of around 4.7 mg L^{-1}).

623 Table 1 Correlations between different relationships that concern changes in DOC or,
624 character of DOC used in this study.

625 Table 2 Median DOC, A254, SUVA and DOC character during the different treatment steps
626 for the period August 2013 to end of May 2014 (5-9 measurements per treatment). Pilot
627 scale sampling sites in brackets (NF permeate (NF-P), activated carbon filtrate for pilot
628 column fed with NF permeate (CF2), activated carbon filtrate for pilot column fed with
629 rapid sand filtrate from the full scale process (CF4) and concentrate from the NF NF-C).

630 Table 3 Median and standard deviation for fluorescence derived data of raw and processed
631 water (SF = sand filtrate, NF-P = NF permeate). Indices from differential EEMs (Raw/SF =
632 coagulation and SF/NF-P = NF) demonstrate characteristics of the removed FDOM. The
633 step NF/CF2 is not included here as DOC is very low and we observed clear trends over
634 time.

635

636

637 Figure A. 1: a: S:can modelled modeled platinum color (mg L^{-1}), b: Time series of S:can
638 modelled DOC (mg L^{-1}) in the raw water (grey), sand filter (black), including measured
639 DOC in raw water (black circles), sand filter (black triangles) and NF permeate (white
640 diamonds for the full pilot study period starting in September 2012 to July 2014. The HW
641 1000 was installed in August 2013. Vertical black lines indicate change of intake depth and
642 hyphenated vertical lines changes in the NF pilot setup. The black horizontal arrow in the
643 lowest panel indicates the nine months experimental period of the HW 1000 nanofilter pilot.

644

645 Figure A. 2: A254 against DOC for all different sampling points. The black hyphenated line
646 indicates the linear relationship ($A254 = -0.0073 + 0.0198 \cdot \text{DOC}$, $r^2 = 0.99$) between A254
647 and DOC after coagulation. The grey arrows indicate either the concurrent removal (NF-P)
648 or increase (NF-C) in A254 with DOC (lower two arrows) during NF. In contrast during
649 coagulation a preferential removal of A254 is observed (upper arrow).

650 Figure A. 3: Amount of HS [ppb] quantified from LC-OCD against measured A254 for all
651 samples. The hyphenated line is the regression curve $\text{HS [ppb]} = 100 + 22900 \cdot A254$; $r^2 =$
652 0.99.

653 Figure A. 4 Typical EEMs for RAW, SF, NF-P and NF permeate followed by active carbon
654 filter water (CF2) displaying data from 2013-08-14 after installation of a fresh active carbon
655 filter (left: raw and processed waters (Raw, SF, NF, CF2 from top to bottom) and right: the
656 removed fraction of FDOM calculated from differential EEMs displaying the amount of

657 FDOM that has been removed during the different treatment steps (Raw-SF, SF-NF, NF-
658 CF2 from top to bottom)

659 Figure A. 5 Predicted concentration of low molecular weight (LMW) neutrals from
660 fluorescence derived parameters humification index (HIX) and freshness index ($\beta:\alpha$) for the
661 NF permeate ($LMW = -16 + 1450 * HIX - 1050 * \beta:\alpha$; $n = 13$; $p < 0.01$)

662 Figure A. 6 Removed DOC over time after change in GAC filter in CF2 and CF4 indicating
663 similar low removal of DOC after just a few months despite different feed DOC
664 concentration.

665 Figure A. 7 Change in median annual ($n=12$) TOC concentration during the period 1996 to
666 2014. The red line describes the change in TOC over time with a slope of $0.12 \text{ mg L}^{-1} \text{ year}^{-1}$
667 $r^2 = 0.56$ and $p < 0.001$.

668 Table A. 1: Median and standard deviation of the different DOC fractions obtained from
669 LC-OCD [ppb] for the period August 2013 to July 2014.

Table 1. Correlations between different relationships that concern changes in DOC or, character of DOC used in this study.

No	Equation
1	$\text{COD}_{\text{Mn}} [\text{mg L}^{-1}] = 0.666 + 5.26 * A_{254}; r^2 = 0.94 \text{ RMSE} = 0.5 [\text{mg L}^{-1}]; n = 115$
2	$\% \text{DOC removed} = 0.788 - 0.00489 * A_{\text{DOS}} [\text{mg L}^{-1}]; r^2 = 0.91 \text{ RMSE} = 1.3\%; n = 249$
3	$\% \text{DOC removed} = 2 - 2.09 * \text{HS}_{\text{frac}}; r^2 = 0.75 \text{ RMSE} = 2.2\%; n = 24$
4	$\text{HS} [\text{ppb}] = 307 + 21800 * A_{254}; r^2 = 0.99 \text{ RMSE} = 200 [\text{ppb}]; n = 29$
5	$\text{SUVA-HS} = 16.2 - 8.19 * \text{FI}; r^2 = 0.93 \text{ RMSE} = 0.17; n = 28$
6	$\text{MW-HS} [\text{Dalton}] = -4190 + 5240 * \text{HIX}; r^2 = 0.80 \text{ RMSE} = 38 [\text{Dalton}]; n = 29$
7	$\text{LMW neutrals} [\text{ppb}] = 124 + 0.489 * \text{Build-Blocks} [\text{ppb}]; r^2 = 0.86, \text{ RMSE} = 99 [\text{ppb}]; n = 29$
8	$\% \text{HS} = 1.52 - 1.33 * \beta; \alpha; r^2 = 0.86, \text{ RMSE} = 0.032; n = 29$

Table 2. Median DOC, A₂₅₄, SUVA and DOC character during the different treatment steps for the period August 2013 to end of May 2014 (5-9 measurements per treatment). Pilot scale sampling sites in brackets (nanofiltration permeate (NF-P), activated carbon filtrate for pilot column fed with NF permeate (CF2), activated carbon filtrate for pilot column fed with rapid sand filtrate from the full scale process (CF4) and concentrate from the nanofiltration NF-C).

Sample	DOC (mg C L ⁻¹)	A ₂₅₄ (m ⁻¹)	SUVA (L mg ⁻¹ m ⁻¹)	%HS	MW _{HS} (Da)	%build	%LMW
Raw	8.8±0.1	26.7±3.5	3.1±0.1	71±3	660±70	3.1	9.4
SF	4.3±0.1	8.9±0.5	2.1±0.1	50±4	450±50	3.6	15.0
NF-P	0.6±0.0	1.1±0.2	1.7±0.3	27±3	420±40	1.4	34.9
CF2 [#]	0.5±0.1	0.5±0.6	1.2±1.3	30±14	420±50	2.1	36.3
NF-C	8.1±0.3	17.4±1.5	2.0±0.2	54±4	450±50	3.3	13.7
CF4 [#]	4.2±0.8	8.4±0.7	2.1±0.2	54±4	450±50	3.2	14.8
DW	4.4±0.2	8.6±0.4	1.9±0.1	52±4	407±60	3.5	15.2

[#]these data have clear trends over time when fresh granular activated carbon is used but are displayed as median values in this table.

Table 3. Median and standard deviation for fluorescence derived data of raw and processed water (SF = sand filtrate, NF-P = nanofiltration permeate). Indices from differential EEMs (Raw/SF = coagulation and SF/NF-P = nanofiltration) demonstrate characteristics of the removed FDOM. The step NF/CF2 is not included here as DOC is very low and we observed clear trends over time.

Sample	FI	HIX	$\beta:\alpha$
Raw	1.48+0.02	0.91+0.01	0.61+0.02
SF	1.68+0.03	0.88+0.01	0.76+0.02
Raw/SF	1.37±0.02	0.94±0.01	0.48±0.01
NF-P	1.84+0.06	0.83+0.02	0.95+0.04
SF/NF-P	1.65±0.02	0.90±0.01	0.70±0.02
CF	1.67 ± 0.03	0.88 ± 0.01	0.75 ± 0.01
SF/CF	1.80 ± 0.25	0.84 ± 0.09	1.07 ± 0.22
DW	1.67 ± 0.03	0.88 ± 0.01	0.75 ± 0.01

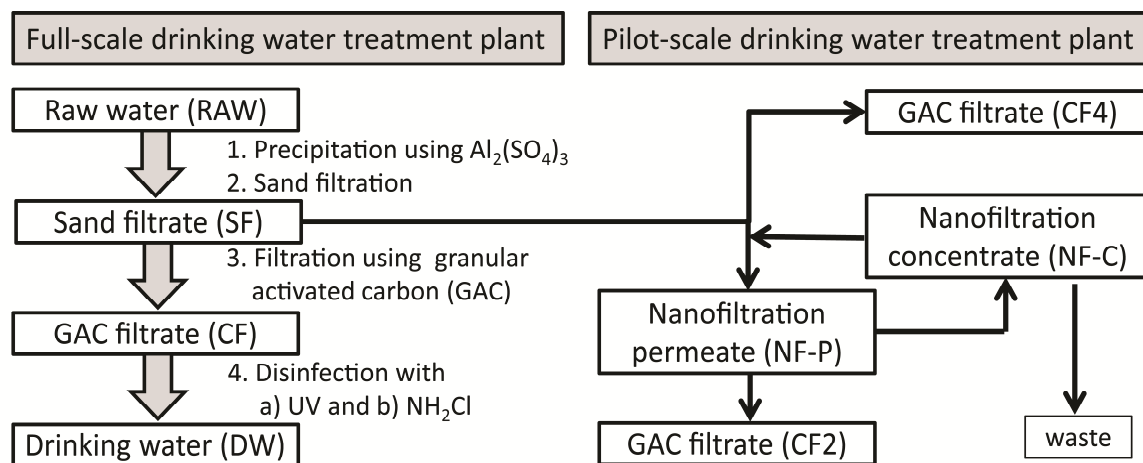


Figure 1. Water treatment train for the full scale drinking water plant and the pilot scale drinking water plant at Görvåln waterworks. The codes for raw water (RAW), sand filter (SF), full scale active carbon filter (CF), nanofilter concentrate (NF-C), nanofilter permeate (NF-P), the other two carbon filters (CF2 and CF4) and drinking water (DW) are used throughout the paper

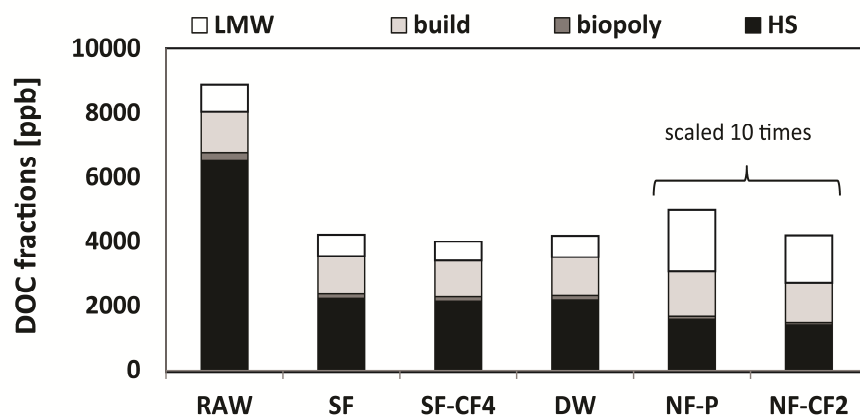


Figure 2. Selected results of median values for changes in DOC [ppb] quantity and quality across the WTP and pilot plant from the raw water (RAW) through the sand filter (SF), the nanofilter (NF-P) and through the full scale activated carbon (SF-CF4) to the final drinking water (DW) and after the activated carbon filter of the pilot plant (NF-CF2) for all samples in the period August 2013 to June 2014. DOC quality parameters in order of decreasing molecular size are codes as biopoly = Biopolymers, HS = Humic substances; LMW = low molecular weight neutrals; build = building blocks.

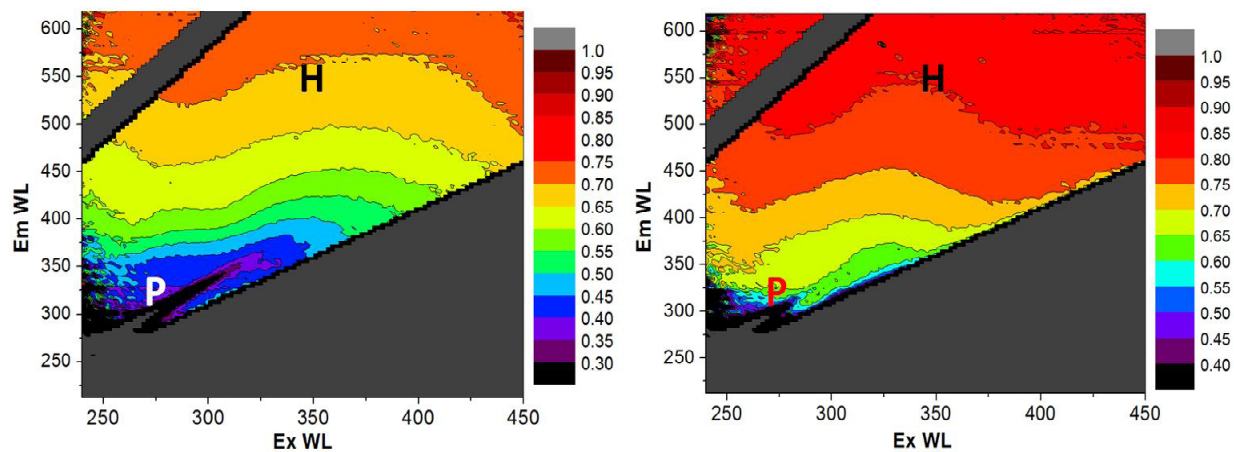


Figure 3: Fraction of removed fluorescent dissolved organic matter for coagulation (left) and NF (right) treatments. Dark red colors indicate strong removal (> 75%) while blue-purple colors indicate less removal (< 40%). The excitation/emission wavelength pairs chosen to represent humic-like (Ex = 350 nm, Em = 550 nm, marked "H" in the EEMs) and protein-like (Ex = 276 nm, Em = 320 nm,

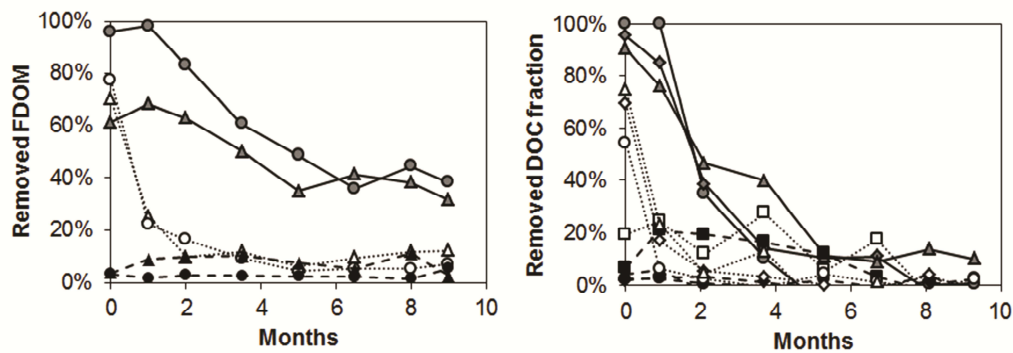


Figure 4 Removal (left panel) of protein-like (triangles) and humic-like (circles) fluorescent dissolved organic matter and (right panel) removal of low molecular neutrals (triangles), humic substances (circles), building blocks (diamonds) and biopolymers (squares) across granulated activated carbon (CF) filters in the full scale treatment (black symbols), as well as the pilot plant reference (CF4, white symbols), and downstream from the NF membrane (CF2, grey symbols).

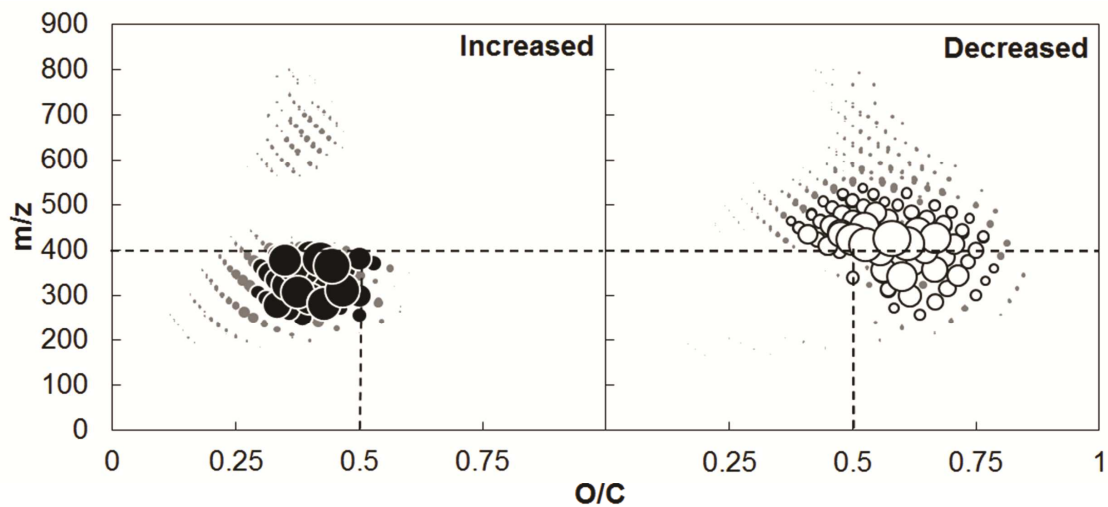


Figure 5: Left: Change in relative abundance as a function of the mass to charge ratio (m/z), left & right = relative change in relative abundance (bubble size) for components that decreased (right, white bubbles) and increased (left, black bubbles) during the pilot scale NF.

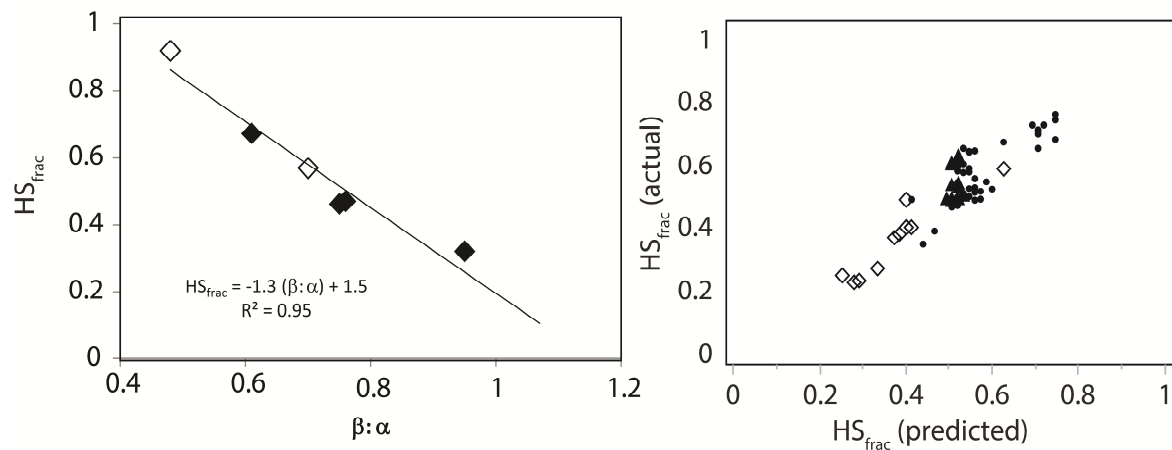


Figure 6: Left: Measured fraction of humic substances (HS_{frac}) for Raw, SF, DW and NF-P as a function of $\beta:\alpha$ (black diamonds) and mass balance derived HS_{frac} for the material that was removed during coagulation and NF treatments versus $\beta:\alpha$ calculated from differential EEM (white diamonds). The regression line is very close to that estimated from all individual data shown to the right. HS_{frac} (predicted) was estimated using $\beta:\alpha$ ($HS_{frac} = 1.52 - 1.33 * \beta:\alpha$) for all samples except CF2 where DOC concentrations were low.

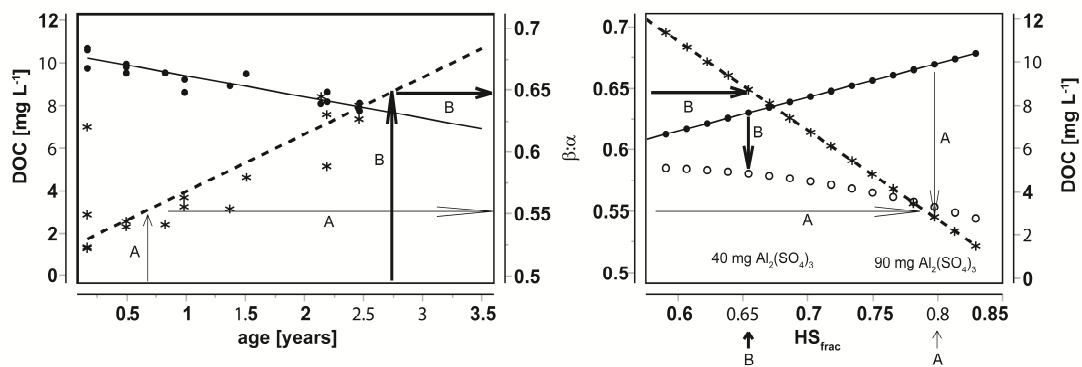


Figure 7: Measured and fitted DOC and $\beta:\alpha$ across Mälaren as a function of water age to the left (Data from Köhler et al 2013). Black circles and black stars display measured DOC and measured $\beta:\alpha$ respectively (left panel). Both DOC and $\beta:\alpha$ are read out as a function of water age (x-axis in left panel) using the horizontally pointing arrows in the left panel. On the right: predicted fraction of DOC composed of HS (HS_{frac}) (x-axis) estimated from as a function of incoming $\beta:\alpha$ (left y-axis) (black stars) and DOC (right y-axis) (black circles) using eqs. 2,3, and 8 in Table A. 1 that relate $\beta:\alpha$, HS, DOC and aluminum dose. Vertically downwards pointing arrows indicate the amount of DOC (difference between black and white circles) that can be removed through coagulation treatment for two different situations (A and B); The predicted outgoing DOC (white circles in the right panel) is illustrated for A (a “young” water 0.7 months of age with high DOC and high $HS_{frac} = 0.8$, requiring around $90 \text{ mg L}^{-1} \text{ Al}_2(\text{SO}_4)_3$ and outgoing DOC of around 3.3 mg L^{-1}) and B (an “old water” with lower DOC, lower $HS_{frac} = 0.65$ leading to a low dose of $40 \text{ mg L}^{-1} \text{ Al}_2(\text{SO}_4)_3$ and outgoing DOC of around 4.7 mg L^{-1}).

Highlights

In this manuscript we document, evaluate and compare the stable performance of a newly developed nanofiltration membrane under a continuous nine month period using a pilot plant with the current full scale treatment in one the largest Swedish water treatment plants in Stockholm.

As we propose to increase the use of spectroscopic techniques, a special effort was put into identifying good spectroscopic proxies for the change in organic matter concentration and character.

We document the performance of the whole treatment train (raw water, coagulation, nanofiltration and active carbon filter both in the pilot and full scale process) with respect to organic matter removal and change in organic carbon character. It is the combination of a number of techniques LC-OCD, high resolution mass spectroscopy and fluorescence spectroscopy that allows us to derive which spectroscopic parameters may be used to control and evaluate the performance of the pilot and full scale plant.

At current full scale operation using aluminum coagulation indicate removal of larger (> 500 Da and HS only) terrestrial ($FI = 1.4$, $\beta:\alpha = 0.5$) and with a higher mean average carbon oxidation state (**Error!** $= 0.5$) carbon. The coupled coagulation-NF pilot plant produced stable outgoing water quality (0.5 mg L^{-1}) during the nine month test trial. The removal of carbon with a much larger range of size (350-500 Da) and properties (**Error!** $= -0.07$, $FI = 1.65$, $\beta:\alpha = 0.5$) during NF as compared to coagulation. Fluorescence derived parameters and correlations are reliable, fast to determine and comparably cheap complement to the more advanced techniques used here (FT-ICR-MS and LC-OCD). DOC removal and change of DOC character in the GAC filters in full scale, the current coagulation scheme and pilot plant setup showed marked differences with slower saturation and larger changes in DOC character using fresh GAC.

Climate change is predicted to change lake water residence time and thus organic carbon character in the lake. Based on the current process scheme we estimate how both factors will effect DOC in the finished water.